Standardized uptake value and radiological density attenuation as predictive and prognostic factors in patients with solitary pulmonary nodules: our experience on 1,592 patients

Duilio Divisi[1], Mirko Barone[1], Luca Bertolaccini[2], Gaetano Rocco[3], Piergiorgio Solli[2], Roberto Crisci[1]; Italian VATS Group*

[1]Thoracic Surgery Unit, University of L'Aquila, "G. Mazzini" Hospital, Teramo, Italy; [2]Thoracic Surgery Unit, ASL Romagna, Forlì, Italy; [3]Thoracic Surgery Unit, National Cancer Institute Pascale Foundation, Napoli, Italy

Contributions: (I) Conception and design: D Divisi, R Crisci, G Rocco; (II) Administrative support: None; (III) Provision of study materials or patients: Italian VATS Group (IV) Collection and assembly of data: None; (V) Data analysis and interpretation: D Divisi, M Barone, P Solli; (VI) Manuscript writing: All authors; (VII) Final approval of manuscript: All authors.

Correspondence to: Duilio Divisi, MD, PhD. Piazza Italia n.1, 64100 Teramo, Italy. Email: duilio.divisi@aslteramo.it.

Background: Multislice computed tomography (MSCT) increased detection of solitary pulmonary nodules (SPNs), changing the management based on radiological and clinical factors. When 18-fluorine fluorodeoxyglucose positron emission tomography combined with computed tomography (^{18}F-FDG-PET/CT) was considered for the evaluation of nodules, the maximum standardized uptake value (SUVmax) more than 2.5 is used frequently as a cut off for malignancy. The purpose of this study is to evaluate SUVmax PET/CT and pulmonary attenuation patterns at MSCT in patients with SPN according to morphological and pathological characteristics of the lesion.

Methods: A retrospective study on 1,592 SPN patients was carried out following approval by the Italian Registry of VATS Lobectomies.

Results: All patients underwent VATS lobectomy. On histologic examination, 98.1% had primary or second metachronous primary lung cancers. In addition, 10.7% presented occult lymph node metastases (pN1 or pN2) on histological examination. Nodule attenuation on CT was associated with the histology of the lesion (p= 0.030); in particular, pure ground glass opacities (pGGOs) and partially solid nodules were related to adenocarcinomatous histotypes. Conversely, a significant relationship between SUVmax and age, nodule size, pathological node status (pN) was found (P=0.007, P=0.000 and P=0.002 respectively).

Conclusions: Nodule attenuation can predict the histology of the lesion whereas SUVmax may relate to the propensity to lymph node metastases.

Keywords: Solitary pulmonary nodule (SPN); maximum standardized uptake value; ground glass opacities; lymph node metastases; lung adenocarcinoma

Introduction

A solitary pulmonary nodule (SPN) is a single radiological, round and well circumscribed pulmonary opacity less than 30 mm in diameter surrounded by aerated, non atelectatic parenchyma and without associated lymph node enlargement, pneumonia and pleural effusions (1). Most SPNs are incidentally found from 0.09% to 7% on chest imaging studies (2). In a report by the Early Lung Cancer Action Project, non-calcified nodules were detected at low-dose chest CT in 23% of the patients (233 of 1,000 patients); malignancy was found in 27 of 1000 patients (2.7%) (3). Expectedly, cancer prevalence varies considerably according to the evaluated population subgroup. In lung cancer
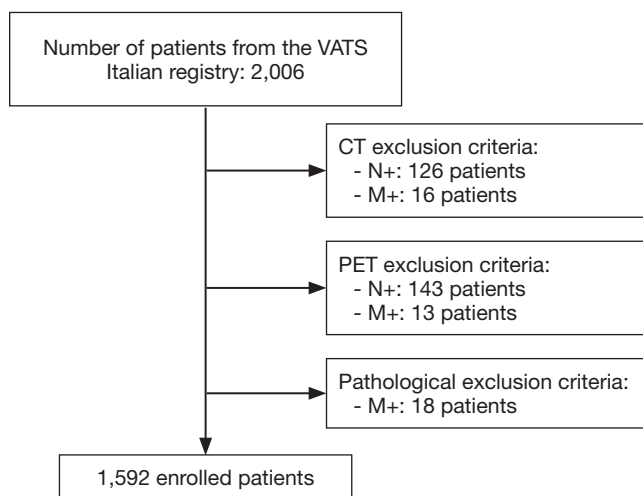
2552

Divisi et al. Predictive impact of imaging of SPN

Figure 1 Inclusion criteria and study design.

screening studies, the malignancy rates range between 2% and 13% reaching up to 82% in high risk patients (4). The widespread use of CT and multislice computed tomography (MSCT) has increased the detection of solid and subsolid nodules. The latter are characterized by a component with higher ground glass attenuation than lung parenchyma but lower than the mediastinal window (5). In addition, subsolid nodules may have a pure ground glass attenuation (pure ground glass opacities, pGGOs) and a mixed solid ground glass attenuation (partially solid ground glass opacities, psGGOs). The etiology of SPNs is broad and includes both benign (such as caused by infection, inflammation or hemorrhage) and malignant disease (such as lung cancer and pulmonary metastases). At high MSCT, there is considerable overlap in the assessment of benign and malignant SPN characteristics (6). However, specific morphological features are useful in determining malignant potential and among these, nodule attenuation is an important morphological pattern. The maximum standardized uptake value (SUVmax) of 18-fluorine fluorodeoxyglucose positron emission tomography combined with computed tomography (^{18}F-FDG-PET/CT) more than 2.5 is used frequently as a cut off for malignancy (7). The aim of this study is to evaluate ^{18}F-FDG-PET/CT SUVmax and MSCT pulmonary density (solid *vs*. subsolid) in SPN patient according to their morphological and pathological patterns, in order to establish the radiological targeted features of malignancy.

Methods

A retrospective study including 2,006 patients with SPN

from January 2014 to May 2016 was carried out after approval by the Italian Registry of VATS Lobectomies. All patients received complete imaging work-up (whole body CT and whole body PET/CT). SPNs were defined as nodules detected in the absence of hilar-mediastinal lymphadenopathy or metastases on CT or PET/CT and in the absence of histopathological diagnosis of metastases (pM+) (*Figure 1*). Eight-hundred ninety-five males and 697 females with a mean age of 67.15±8.90 (range, 22.0–89.0 years) were enrolled. Demographic and clinical data are summarized in *Table 1*. One-thousand ninety-six patients (68.8%) presented at CT a less than 20 mm SPN, with a slight predominance for the right lung (984, 61.8%). Concerning CT nodule attenuation, 1,272 patients (79.9%) showed solid solitary pulmonary nodules (sSPNs), 291 patients (18.3%) psGGOs and 29 patients (1.8%) a pGGOs. The mean SUVmax was 4.11±4.80 (range, 0–31). Preoperative histological assessment was attempted by fine-needle aspiration biopsy (FNAB) in 892 patients (56.03%), endobronchial ultrasound biopsy (EBUS) in 27 patients (1.69%) and endoscopic ultrasonography (EUS) in 1 (0.06%), with a detection rate of 79.37% (708 out of 892), 37.03% (10 of 27) and 0% (0 of 1), respectively. Statistical analysis was performed using SPSS version 20.0 software for Windows (IBM, Chicago, USA). Continuous variables were expressed as absolute value, simple percentages, means and standard deviations, whereas categorical ones in terms of frequency and percentage. Statistical differences or correlations between cohorts were evaluated with Spearman's correlation both for categorical and continuous variables, while for multivariate analysis unpaired t-test and Mann-Whitney U-test were evaluated. All risk factors were correlated with SUVmax, histology and lymph node status (N) using both bivariate and multivariate analysis and a P value <0.05 was considered statistically significant.

Results

All 1,592 patients underwent VATS lobectomy; a complete hilar-mediastinal lymphadenectomy was added in 1,120 (70.4%). On histologic examination, 98.1% (1,562 patients) had primary or secondary lung cancers and 1.9% (30 patients) had a benign disease. Primary adenocarcinoma was the predominant histotype (1,097, 68.9%), followed by other carcinomas and neuroendocrine tumors (12.8% and 10.2%, respectively). In addition, 10.7% presented occult lymph node metastases (pN1 or pN2) on histologic evaluation. Furthermore, lymph node micrometastases were reported

Table 1 SPN population: demographic, radiological and pathological characteristics

Clinical data	N	%	Mean	Interval	SD
Gender					
Male	895	56.2			
Female	697	43.8			
Age			67.15	22.0–89.0	8.90
Nodule size (CT)					
<20 mm	1,096	68.8			
20–30 mm	496	31.2			
Nodule side (CT)					
Right	984	61.8			
Left	608	38.2			
Nodule density (CT)					
Solid	1,272	79.9			
Partially solid GGO	291	18.3			
Pure GGO	29	1.8			
SUVmax (PET)			4.11	(0–31.0)	4.80
Preoperative histology					
Yes	718	45.1			
No	874	54.9			
Type of lesion					
Benign	30	1.9			
Malignant	1,562	98.1			
Histology cohorts					
Benign diseases	30	1.9	(TBC n.3, Pseudotumor n.4, Other inflammatory diseases n.7, Hamartoma n.9, Hamartochondroma n.7)		
Adenocarcinomas	1,097	68.9	(AAH n.29, AIS n.35, MIA n.164, Invasive adenocarcinoma n. 857, Adenoidocystic carcinoma n.12)		
Carcinomas	204	12.8	(Squamous carcinoma n.203)		
Neuroendocrine tumors	162	10.2	(Typical carcinoid n.91, Atypical carcinoid n.52, Large cell carcinoma n.14, SCLC n.5)		
Other primary neoplasms	27	1.7	(Lymphoma n.6, Carcinosarcoma n.2, NSCLC NAS 19)		
Metastases	72	4.5			
Surgical approach					
Anterior according Copenhagen	1,203	75.6			
Anterior according D'Amico	182	11.4			
Lateral according McKenna	76	4.8			
Posterior according Walker	3	0.2			
Totally endoscopic according Gossot	31	1.9			
Uniportal according Gonzalez Rivas	97	6.1			
Conversion	129	8.1			

Table 1 (*continued*)

2554

Divisi et al. Predictive impact of imaging of SPN

Table 1 (*continued*)

Clinical data	N	%	Mean	Interval	SD
Type of resection					
Upper lobectomy	912	57.3			
Middle lobectomy	127	8.0			
Lower lobectomy	538	33.8			
Upper bilobectomy	8	0.5			
Lower bilobectomy	7	0.4			
LN dissection	1,577	99.1			
LND type					
RND	1,120	70.4			
Sampling	457	28.7			
N resected LN			13.33	(0–64.0)	7.93
N status					
N0	1,392	87.4			
N1	92	5.8			
N2	78	4.9			
N micrometastases	48	3.0			

SPN, solitary pulmonary nodule; CT, computed tomography; GGO, ground glass opacities; PET, positron emission tomography; LN, lymph node; LND, lymph node dissection; RND, radical node dissection.

in 3.0% (*Table 1*). Bivariate analysis between independent factors and SUVmax is reported in *Table 2* while the correlation between independent factors, histology and SUVmax is described in *Table 3*. Nodule attenuation on CT was associated with the nature of lesion (P=0.030). In particular, pGGOs and partially solid nodules were related to adenocarcinomatous histotypes with different statistical strength (*Figure 2*). Specifically, pre-invasive lesions [such as atypical adenomatous hyperplasia (AAH) and adenocarcinoma *in situ* (AIS)] occurred preferentially as psGGOs while minimally invasive or invasive ones were detected as solid nodules (*Table 4*). Finally, the same nodule attenuation on CT presented a strong statistical correlation with the propensity for lymph node metastasis (P=0.000), albeit the comparison of pGGOs to solid nodules did not confirm these findings. In fact, the involvement of the N1 and the N2 compartments were noted in 5.58% and 3.48% in pGGO and psGGO patients, respectively (*Table 5*).

Discussion

From a clinical standpoint, the management of SPN is controversial (4,5,8-11). Imaging with ^{18}F-FDG-PET is a well-established indication for the evaluation of SPNs. In current practice, a semi-quantitative determination of FDG avidity calculated by standard uptake value in a region of interest (ROI) is the most common method to assess pulmonary nodules. FDG uptake on PET can be qualitatively and semi-quantitatively evaluated. Visual assessment is based upon comparison between FDG lesion uptake and mediastinum (12), but nodules with similar FDG uptake to the mediastinal pool are challenging; for these reasons, a 2.5 cut off the SUVmax has been used for the establishment of malignancy. However, FDG and its avidity is not tumor-specific and an increased uptake is reported in benign diseases (13-16). On the other hand, malignancies can be poorly avid leading to mistaken conclusions or interpretation of findings (17-19). In addition, it must be considered that many factors influence the SUV such as ROI itself, volume effects and corrections, reconstruction methods and body size (20). The combination of computed tomography and PET showed an excellent performance in the SPN classification (4,21). In this setting, the results of the present study indicate that there is a correlation between the nodule size and the SUVmax value (P=0.000) which is consistent with the conclusions by Khalaf *et al.* (22).

Table 2 Bivariate analysis (Spearman's correlation) between independent factors and SUVmax in solitary pulmonary nodule patients

Factor	SUVmax	
	Spearman R	P
Age*	0.068	0.007
Nodule size CT**	0.164	0.000
Nodule density CT**	0.041	0.102
Stage**	−0.003	0.918
Type of lesion**	−0.021	0.418
N status**	0.077	0.002
Number of resected LN*	−0.092	0.103
LN micrometastases**	−0.083	0.167

*, continuous variable; **, catgorical variable. CT, computed tomography; LN, lymph node.

Reasons are to be found in the nodule diameter which influences SUV; in fact, small benign pulmonary nodules can present average SUV similar to malignant ones. Moreover, a 2.5 SUVmax threshold in small nodules can lead to false positive PET scans. In our study, the SUVmax was 3.300±3.303 for benign diseases, 3.25±4.01 for invasive adenocarcinomas and 6.51±6.26 for squamous carcinomas; no malignant nodules presented a mean SUVmax of less than 2.5. Furthermore, we noticed two interesting relationships: (I) in a fashion similar to the results presented by Nahmias et al. (23), we found a significant correlation between SUVmax and patients' age (P= 0.016); (II) in agreement with Xu et al. (24), we also observed a significant correlation between SUVmax and prediction of lymph node metastases on histological specimens (P=0.001). Lin et al. (25) recently reported 284 consecutive cN0 patients with peripheral NSCLC who underwent PET/CT scans followed by pulmonary resections in order to identify predictors of occult lymph node metastases. In 8.5% lung cancers diagnosed N0 by PET/CT, the Authors revealed pathological N2 metastases and the SUVmax was the unique independent risk factor for occult N2 disease (25). Similar results were reported by Park et al. (26) in patients with less than 30 mm NSCLC, confirming SUVmax as a useful predictive marker for tumor aggressiveness. According to our inclusion criteria (cN0 and cM0), the only independent variable affecting staging is T value. This parameter is function of the nodule's size (27) according to which all malignant solitary nodules would be pT1 (T1a and T1b).

However, assuming this criterion as constant, the only interfering variable would be the topographic aspect. In fact, in the staging process, the T component increases as it is located either distal (T3 pleurae) or proximal to the hilum (T2b main bronchus or T4 mediastinum). For these reasons, the correlation between the changes in staging and the SUVmax values would only be an expression of different positions and relationships of the nodule itself. In our study, we showed no overall significant correlation between histological findings and SUVmax (P=0.586). Davidson et al. (28) suggested that squamous pulmonary carcinoma presented a significantly greater uptake on PET/CT than adenocarcinoma. We found a mean SUVmax of 6.51±6.26 for squamous carcinomas and of 4.63±3.97 for adenocarcinomas (both pre-invasive and invasive patterns; P=0.132). On the other hand, considering only the squamous carcinoma and invasive adenocarcinoma, a significant difference was noted (P=0.013) whereas when only adenocarcinoma subtypes were considered, no statistical correlation in SUVmax was found (P=0.324). In particular, contrary to what already presented in the literature, AAH, AIS and minimally invasive adenocarcinoma (MIA) presented higher uptake values rather than invasive adenocarcinomas (4.86, 5.00, 5.42 and 3.25, respectively). Chiu et al. (29), in a study on 142 patients with 153 lung primary adenocarcinomas, showed that FDG uptake differs according to various histological subtypes of lung adenocarcinoma due to differences in GLU-1 expression. Nakamura et al. (30), in a study on 255 patients, also reported similar results concluding that SUVmax was closely associated with histologic subtype in resected adenocarcinoma specimens. Specifically, pre-invasive lesions (such as AAH and AIS) occurred as ground glass opacities, while invasive ones were detected as solid nodules. These changes would seem therefore to correlate with the cytoarchitectonic reorganization of malignant SPNs from pre-invasive to invasive forms. Kobayashi et al. (31), in a review on ground glass opacities, also showed that atypical adenomatous hyperplasia and adenocarcinoma in situ typically develop as pure GGOs, whereas more advanced adenocarcinomas may include a larger solid component within the GGO region. Similar trends were also reported between density of lesion and propensity for lymph node metastases (P=0.000). In particular, pGGOs did not present propensity to node metastases when compared to solid nodules. Ye et al. (32), retrospectively analyzed a series of 271 patient with small nodules of peripheral lung adenocarcinoma and were able

2556

Divisi et al. Predictive impact of imaging of SPN

Table 3 Multivariate analysis between independent factors and SUVmax in solitary pulmonary nodule patients

Subjects	N	Mean	SD	CI 95%		P
				Min	Max	
Age[a]	1,592	67.14	8.891	65.71	66.58	0.000
Nodule size CT[a]						0.000
<20 mm	1,096	3.48	4.191	3.23	3.73	
20–30 mm	496	5.59	5.684	4.99	5.99	
Nodule density CT[b]						0.107
Solid	1,272	4.12	4.939	3.84	4.39	
psGGO	291	4.24	4.230	3.76	4.73	
pGGO	29	2.28	3.316	1.01	3.54	
Stage[b]						0.081
IA	1,429	4.06	4.708	3.82	4.30	
IB	95	4.14	5.760	2.96	5.31	
IIA	4	10.25	8.655	−3.52	24.02	
IIB	29	5.10	4.923	3.23	6.98	
IIIA	5	5.40	3.975	0.46	10.34	
Type of lesion[a]						0.353
Benign	30	3.30	3.303	3.23	3.73	
Malignant	1,562	4.12	4.820	4.99	5.99	
N status[b]						0.004
N0	1,392	3.99	4.727	3.74	4.23	
N1	92	4.97	5.562	3.82	6.12	
N2	78	5.55	5.244	4.37	6.73	
LN micrometastases[a]						0.223
Yes	48	4.94	5.583	3.32	6.56	
No	1,544	4.08	4.769	3.84	4.32	

[a], unpaired t-test (χ^2); [b], Mann-Whitney U-test. CT, computed tomography; psGGO, partially solid ground glass opacities; pGGO, pure ground glass opacities; LN, lymph node.

to demonstrate a significant difference in lymph node metastasis between the aforesaid cohorts concluding that pure GGOs were not associated to lymph node metastasis. Moreover, Kim *et al.* (33) emphasized the low incidence of lymph node (n. 2, 2.25%) and distant metastases (n. 3, 3.37%) in evaluating 89 patients with 134 pGGNs. According to these results, Ye *et al.* (34) recently suggested to avoid lymph node dissection in lung adenocarcinoma pure GGO cT1aN0M0 patients. In our study, the limitations are two-fold: (I) this is a non homogeneous series from a national wide registry of "VATS Lobectomies" performed for both benign and malignant conditions; (II) no control group could be established.

Conclusions

SPNs are clinically challenging and their management is affected by the probability of malignancy defined according to history, morphological and radiological features. In fact, nodules attenuation, double-volume time and standardized uptake value may entail important predictive and prognostic significance. In particular, we found that SUVmax was positively correlated with the potential for lymphatic metastasis and the clinical stage. On the other hand, the nodules attenuation patterns should be carefully considered especially when evaluating sub solid nodules as their variation could be an expression of neoplastic progression.
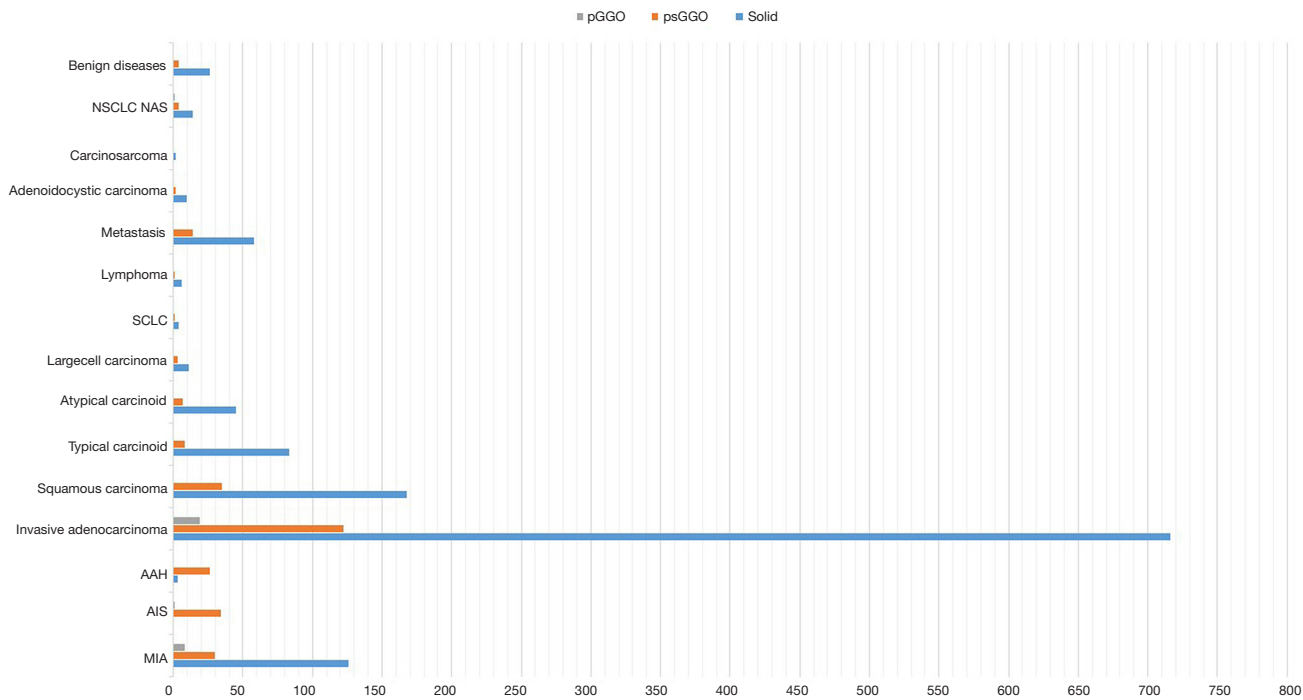
Figure 2 Nodule attenuation pattern *vs.* histology in solitary pulmonary nodule patients (simple bar plot): pulmonary subsolid nodules usually relate to adenocarcinomatous pattern.

Table 4 Histological specimen *vs.* nodule attenuation pattern at CT

Histological specimen	Nodule density CT			Total
	Solid	Partially solid GGO	Pure GGO	
MIA	126	30	8	164
AIS	0	34	1	35
AAH	3	26	0	29
Invasive adenocarcinoma	716	122	19	857
Squamous carcinoma	168	35	0	203
Typical carcinoid	83	8	0	91
Atypical carcinoid	45	7	0	52
Large cell carcinoma	11	3	0	14
SCLC	4	1	0	5
Lymphoma	6	1	0	7
Metastasis	58	14	0	72
Adenoidocystic carcinoma	10	2	0	12
Carcinosarcoma	2	0	0	2
NSCLC NAS	14	4	1	19
Benign diseases	26	4	0	30

CT, computed tomography; GGO, pure ground glass opacities; MIA, minimally invasive adenocarcinoma; AIS, and adenocarcinoma *in situ*; AAH, atypical adenomatous hyperplasia.

Table 5 Nodule attenuation gradient at CT *vs.* propensity to lymph node metastases in SPN patients

Nodule density CT	N			Total	P
	0	1	2		
Solid	1,102	76	68	1,246	0.000
Partially solid GGO	261	16	10	287	
Pure GGO	29	0	0	29	
Total	1,392	92	78	1,562	

CT, computed tomography; SPN, solitary pulmonary nodule; GGO, pure ground glass opacities.

The only bias of our study is the rigid preoperative lung cancer selection of patients that reduced futile thoracotomies below 10–30% of the cases reported in the literature.

Acknowledgements

None.

Footnote

Conflicts of Interest: The authors have no conflicts of interest to declare.

2558

Divisi et al. Predictive impact of imaging of SPN

Ethical Statement: This study received ethical approval (number 81/2014/O/Oss in date 2014-05-13) from the Independent Ethics Committee of S. Orsola-Malpighi Hospital, Bologna University (Italy).

*, Italian VATS Group collaborator list: Duilio Divisi, MD PhD (Università dell'Aquila, L'Aquila); Mirko Barone, MD (Università dell'Aquila, L'Aquila); Luca Bertolaccini, MD PhD (AUSL Romagna Teaching Hospital, Forlì); Gaetano Rocco, MD PhD (National Cancer Institute – Pascale Foundation, Napoli); Piergiorgio Solli, MD PhD (AUSL Romagna Teaching Hospital, Forlì); Roberto Crisci, MD PhD (Università dell'Aquila, L'Aquila); Alessandro Bertani, MD (IRCCS ISMETT, Palermo); Alessandro Gonfiotti, MD (Careggi Hospital, Firenze); Mario Nosotti, MD (Policlinico Ca'Granda, Milano); Andrea Droghetti, MD (ASST Mantova-Cremona, Mantova); Carlo Curcio, MD (Monaldi Hospital, Napoli); Dario Amore, MD (Monaldi Hospital, Napoli); Giuseppe Marulli, MD (University of Padova); Samuele Nicotra, MD (University of Padova); Andrea De Negri, MD (San Martino Hospital, Genova); Paola Maineri, MD (San Martino Hospital, Genova); Gaetano di Rienzo (Vito Fazzi Hospital, Lecce); Camillo Lopez, MD (Vito Fazzi Hospital, Lecce); Angelo Morelli, MD (S. Maria delle Misericordia Hospital, Udine); Francesco Londero, MD (S. Maria delle Misericordia Hospital, Udine); Lorenzo Spaggiari, MD (IEO Hospital, Milano); Roberto Gasparri, MD (IEO Hospital, Milano); Guido Baietto, MD (Maggiore della Carità Hospital, Novara); Caterina Casadio, MD (Maggiore della Carità Hospital, Novara); Maurizio Infante, MD (Borgo Trento Hospital, Verona); Cristiano Benato, MD (Borgo Trento Hospital, Verona); Marco Alloisio, MD (IRCCS Humanitas, Milano); Edoardo Bottoni, MD (IRCCS Humanitas, Milano); Giuseppe Cardillo, MD (Forlanini Hospital, Roma); Francesco Carleo, MD (Forlanini Hospital, Roma); Franco Stella, MD (S. Orsola Hospital, Bologna); Giampiero Dolci, MD (S. Orsola Hospital, Bologna); Francesco Puma, MD (University of Perugia); Damiano Vinci, MD (University of Perugia); Giorgio Cavallesco, MD (University of Ferrara); Pio Maniscalco, MD (University of Ferrara); Luca Ampollini, MD (University of Parma); Paolo Carbognani, MD (University of Parma); Alberto Terzi, MD (Negrar Hospital, Verona); Andrea Viti, MD (Negrar Hospital, Verona); Giampiero Negri, MD (S. Raffaele Hospital, Milano); Alessandro Bandiera, MD (S. Raffaele Hospital, Milano); Reinhold Perkmann, MD (Bolzano Hospital, Bolzano); Francesco Zaraca, MD (Bolzano Hospital, Bolzano); Claudio Andretti, MD (S. Andrea Hospital, Roma); Camilla Poggi, MD (S. Andrea Hospital, Roma); Felice Mucilli, MD (S. Maria Annunziata Hospital, Chieti); Pierpaolo Camplese, MD (S. Maria Annunziata Hospital, Chieti); Luca Luzzi, MD (University of Siena); Marco Ghisalberti, MD (University of Siena); Andrea Imperatori, MD (University of Varese); Nicola Rotolo, MD (University of Varese); Luigi Bortolotti, MD (Humanitas Gavazzeni Hospital, Bergamo); Giovanna Rizzardi, MD (Humanitas Gavazzeni Hospital, Bergamo); Massimo Torre, MD (Niguarda Hospital, Milano); Alessandro Rinaldo, MD (Niguarda Hospital, Milano); Armando Sabbatini, MD (Ospedali Riuniti, Ancona); Majed Refai, MD (Ospedali Riuniti, Ancona); Mauro Roberto Benvenuti, MD (Spedali Civili, Brescia); Diego Benetti, MD (Spedali Civili, Brescia); Alessandro Stefani, MD (Ospedale Policlinico, Modena); Pamela Natali, MD (Ospedale Policlinico, Modena); Paolo Lausi, MD (Ospedale Molinette, Torino); Francesco Guerrera, MD (Ospedale Molinette, Torino)

References

1. Ost D, Fein AM, Feinsilver SH. Clinical practice. The solitary pulmonary nodule. N Engl J Med 2003;348:2535-42.
2. Murrmann GB, van Vollenhoven FH, Moodley L. Approach to a solid solitary pulmonary nodule in two different settings-"Common is common, rare is rare". J Thorac Dis 2014;6:237-48.
3. Henschke CI, McCauley DI, Yankelevitz DF, et al. Early Lung Cancer Action Project: overall design and findings from baseline screening. Lancet 1999;354:99-105.
4. Gould MK, Fletcher J, Iannettoni MD, et al. Evaluation of patients with pulmonary nodules: when is it lung cancer?: ACCP evidence-based clinical practice guidelines (2nd edition). Chest 2007;132:108S-130S.
5. Naidich DP, Bankier AA, MacMahon H, et al. Recommendations for the management of subsolid pulmonary nodules detected at CT: a statement from the Fleischner Society. Radiology 2013;266:304-17.
6. Lee HY, Lee KS. Ground-glass opacity nodules: histopathology, imaging evaluation, and clinical implications. J Thorac Imaging 2011;26:106-18.
7. Grgic A, Yüksel Y, Gröschel A, et al. Risk stratification of solitary pulmonary nodules by means of PET using (18) F-fluorodeoxyglucose and SUV quantification. Eur J Nucl Med Mol Imaging 2010;37:1087-94.
8. Callister ME, Baldwin DR, Akram AR, et al. British Thoracic Society guidelines for the investigation and management of pulmonary nodules. Thorax 2015;70 Suppl 2:ii1-ii54.
9. Bach PB, Silvestri GA, Hanger M, et al. ACCP evidence-

based clinical practice guidelines - 2nd ed. Chest 2007;132:69S77S.

10. MacMahon H, Austin JH, Gamsu G, et al. Guidelines for management of small pulmonary nodules detected on CT scans: a statement from the Fleischner Society. Radiology 2005;237:395-400.

11. Sim YT, Poon FW. Imaging of solitary pulmonary nodule-a clinical review. Quant Imaging Med Surg 2013;3:316-26.

12. Herder GJ, van Tinteren H, Golding RP, et al. Clinical prediction model to characterize pulmonary nodules: validation and added value of 18F-fluorodeoxyglucose positron emission tomography. Chest 2005;128:2490-6.

13. Lee KS, Kim Y, Han J, et al. Bronchioloalveolar carcinoma: clinical, histopathologic, and radiologic findings. Radiographics 1997;17:1345-57.

14. Heyneman LE, Patz EF. PET imaging in patients with bronc hioloalveolarcellcarcinoma. Lung Cancer 2002;38:261-6.

15. Erasmus JJ, McAdams HP, Patz EF Jr, et al. Evaluation of primary pulmonary carcinoid tumors using FDG PET. AJR Am J Roentgenol 1998;170:1369-73.

16. Ollenberger GP, Knight S, Tauro A. False-positive FDG positron emission tomography in pulmonary amyloidosis. Clin Nucl Med 2004;29:657-8.

17. Kapucu LO, Meltzer CC, Townsend DW, et al. Fluorine-18-fluorodeoxyglucose uptake in pneumonia. J Nucl Med 1998;39:1267-9.

18. Nomori H, Watanabe K, Ohtsuka T, et al. Evaluation of F-18 fluorodeoxyglucose (FDG) PET scanning for pulmonary nodules less than 3 cm in diameter, with special reference to the CT images. Lung Cancer 2004;45:19-27.

19. Chen CJ, Lee BF, Yao WJ, et al. Dual-phase 18F-FDG PET in the diagnosis of pulmonary nodules with an initial standard uptake value less than 2.5. AJR Am J Roentgenol 2008;191:475-9.

20. Thie JA. Understanding the standardized uptake value, its methods, and implications for usage. J Nucl Med 2004;45:1431-4.

21. Kim SK, Allen-Auerbach M, Goldin J, et al. Accuracy of PET/CT in characterization of solitary pulmonary lesions. J Nucl Med 2007;48:214-20.

22. Khalaf M, Abdel-Nabi H, Baker J, et al. Relation between nodule size and 18F-FDG-PET SUV for malignant and benign pulmonary nodules. J Hematol Oncol 2008;1:13.

23. Nahmias C, Wahl LM. Reproducibility of standardized uptake value measurements determined by 18F-FDG PET in malignant tumors. J Nucl Med 2008;49:1804-8.

24. Xu ZQ, Xie LJ, Fan W, et al. Risk factors for mediastinal lymph node metastasis in non-small-cell lung cancer by PET/CT. Nucl Med Commun 2014;35:466-71.

25. Lin JT, Yang XN, Zhong WZ, et al. Association of maximum standardized uptake value with occult mediastinal lymph node metastases in cN0 non-small cell lung cancer. Eur J Cardiothorac Surg 2016;50:914-9.

26. Park SY, Yoon JK, Park KJ, et al. Prediction of occult lymph node metastasis using volume-based PET parameters in small-sized peripheral non-small cell lung cancer. Cancer Imaging 2015;15:21.

27. American Joint Committee on Cancer. Lung. AJCC Cancer Staging Manual. 7th ed. New York: Springer. 2010:253-66.

28. Davidson JA, Wong V, Fraser R, et al. Comparison of primary tumor maximal standardized uptake value (SUVmax) on preoperative [18F]fluorodeoxyglucose positron emission tomography/computed tomography (PET/CT) and histological subtype in patients with non-small cell lung cancer (NSCLC). J Clin Oncol 2009;27:abstr 7571.

29. Chiu CH, Yeh YC, Lin KH, et al. Histological subtypes of lung adenocarcinoma have differential 18F-fluorodeoxyglucose uptakes on the positron emission tomography/computed tomography scan. J Thorac Oncol 2011;6:1697-703.

30. Nakamura H, Saji H, Shinmyo T, et al. Close association of IASLC/ATS/ERS lung adenocarcinoma subtypes with glucose-uptake in positron emission tomography. Lung Cancer 2015;87:28-33.

31. Kobayashi Y, Mitsudomi T. Management of ground-glass opacities: should all pulmonary lesions with ground-glass opacity be surgically resected? Transl Lung Cancer Res 2013;2:354-63.

32. Ye B, Feng J, Pan XF, et al. Correlation analysis between imaging features and lymph node metastasis in T1a lung adenocarcinoma. Zhonghua Wai Ke Za Zhi 2013;51:904-7.

33. Kim TJ, Park CM, Goo JM, et al. Is there a role for FDG PET in the management of lung cancer manifesting predominantly as ground-glass opacity? AJR Am J Roentgenol 2012;198:83-8.

34. Ye B, Cheng M, Ge XX, et al. Factors that predict lymph node status in clinical stage T1aN0M0 lung adenocarcinomas. World J Surg Oncol 2014;12:42.